

LA-UR-71-3260

TITLE: Design of a 20-MJ Superconducting Ohmic-Heating Coil

AUTHOR(S): S. K. Singh, J. H. Murphy, M. A. Janocko,
 H. E. Haller, D. C. Litz, and P. W. Eckels
 Westinghouse Electric Corporation
 Pittsburgh, PA 15235

J. D. Rogers and P. Thullen, CTR-9

SUBMITTED TO: 8th Symposium on Engineering Problems
 of Fusion Research, November 1979,
 San Francisco, CA

CTR

DISCLAIMER

By acceptance of this article, the publisher recognizes that the U.S. Government retains a non-exclusive, royalty-free license to publish or reproduce the published form of this contribution, or to allow others to do so, for U.S. Government purposes.

The Los Alamos Scientific Laboratory requests that the publisher identify this article as work performed under the auspices of the Department of Energy.



los alamos
 scientific laboratory
 of the University of California
 LOS ALAMOS, NEW MEXICO 87545

An Affirmative Action/Equal Opportunity Employer

Paper No. 14-09

DESIGN OF A 20 MJ SUPERCONDUCTING OHMIC-HEATING COIL

S. K. Singh, J. H. Murphy, M. A. Janocko, H. E. Haller, D. C. Litz, and P. W. Eckels

WESTINGHOUSE ELECTRIC CORPORATION
PITTSBURGH, PA. 15235

J. D. Rogers and P. Thullen

LOS ALAMOS SCIENTIFIC LABORATORY
LOS ALAMOS, N.M. 87544

Prepared for
IEEE
8th Symposium on Engineering Problems
of Fusion Research

November 1979

DESIGN OF A 20 MJ SUPERCONDUCTING OHMIC-HEATING COIL*

S. K. Singh, J. H. Murphy, M. A. Janocko, H. E. Haller, D. C. Litz and P. W. Eckels
Westinghouse Electric Corporation, Pittsburgh, PA. 15235

J. D. Rogers and P. Thullen,
Los Alamos Scientific Laboratory, Los Alamos, N.M. 87544

Summary

Conceptual designs of 20-MJ superconducting coils which were developed to demonstrate the feasibility of an ohmic-heating system are discussed. The superconductor materials were NbTi and Nb₃Sn for the pool boil and forced-flow cooling, respectively. The coils were designed to be cryostable for bipolar operation from +7 to -7 tesla maximum field within one second. The structural design addresses the distribution of structure and structural materials used in the pulsed field environment. The cyclic stresses anticipated and the fatigue limits of the structural materials were examined in view of the operating life of the coil. The coils were designed to generate the flux swings while simultaneously meeting the limitations imposed by cooling, insulation, current density and the stresses in the materials. Both the pool and forced cooled conductors have the same criterion for cryostability, i.e., the conductor must return to the superconducting state from an initial temperature of 20K while the full transport current is flowing through the conductor.

Introduction

A full-scale Tokamak reactor will require considerable development of various components before they can be viable. Among the components to be developed are those for the poloidal field systems. Studies of the Tokamak poloidal field systems requirements have been in progress at LASL (Los Alamos Scientific Laboratory) for several years. The principal functions of the poloidal field coil system in a Tokamak are to hold the plasma in proper position and to supply the initial plasma heating. The conditions which will be imposed upon the ohmic-heating coils will be very demanding, particularly the central solenoid. These coils must be operated in the bipolar mode, undergoing a complete field and current reversal, and are in the maximum field to be experienced by a winding. The current swing requirement is made somewhat difficult by the eddy current loss due to the changing magnetic field.

This paper presents the results of a study⁽¹⁾ performed by the Westinghouse Electric Corporation in 1978 for LASL to demonstrate the feasibilities of a superconducting ohmic-heating coil. Since the completion of the study the Westinghouse Electric Corporation has been involved with the detail design and analysis of a 20-MJ superconducting ohmic-heating coil for LASL under a separate contract. The results of the detailed design phase of the program will be reported later.

Design Requirements

The specified magnet performance requirements and operating environment are summarized below⁽¹⁾.

- Energy storage of 20 MJ
- Both immersion cooled and force flow cooled coils
- NbTi or Nb₃Sn superconductors
- Bipolar operation from +7 tesla to -7 tesla maximum fields
- Bipolar, half cycle sinusoidal operation from full positive field to full negative field within 1 second
- Discharge into a resistive load for a 0.5 second e-folding time
- Hold time between field reversal to range from 10 seconds to 100 seconds at full field
- Cryostable coil, coil is not to go normal during operation simulating above conditions
- 50 kA conductor current
- Current source and transfer power supplies will be a 12-phase, 62 kA solid state power supply; and a 20 MJ, 2 kV, 62 kA 0.5 second discharge homopolar machine.

The development of the conceptual designs have been an iterative process of design, evaluation and modification, resulting in concepts that meets all the operating requirements. The stored energy requirement, operating current density and the desire for a fully ventilated coil resulted in a multilayer helically wound coil design. The selection of this design concept was influenced by the unique success of the Westinghouse 300 kJ coil⁽²⁾ tested at LASL when subjected to an ohmic-heating cycle⁽³⁾.

Four conductors were designed for potential application in a pool-cooled ohmic-heating (OH) coil. Two superconducting materials were considered: NbTi and Nb₃Sn. For each material a cabled conductor with 504 strands such as the one illustrated in Figure 1 and a lattice braided conductor⁽⁴⁾ with 503 strands such as the one shown in Figure 2 were considered. All conductors were designed to be cryostable, i.e., the heat generation rate when all of the current is in the stabilization material is less than the heat removal rate. The heat removal rate, or recovery heat flux,

*Work supported by University of California,
Los Alamos Scientific Laboratory, Contract No.
L48-8407C-1

$\left(\frac{S_a}{S_t}\right) = \frac{1}{3}$ and for an uncompacted lattice braid conductor $\left(\frac{S_a}{S_t}\right) = 1$

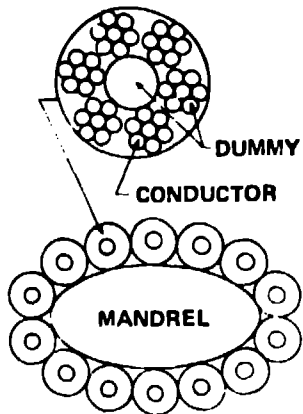


Figure 1 504 Strand Cabled Conductor

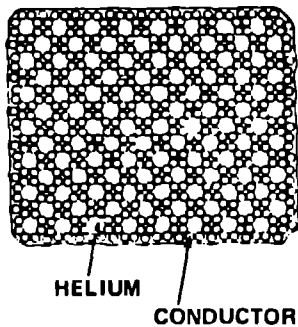


Figure 2 503 Strand Lattice Braid Conductor

q_c , which the pool-cooled conductors were designed to meet is 0.2 W/cm^2 . The copper to non-copper ratio and the strand diameter were selected to give an operating-current-density to critical-current-density ratio, j/j_c , approximately equal to 0.5 and an overall conductor current, I , equal to 50,000 A.

The strand diameter, d , and the copper to non-copper ratio, are determined by simultaneous solution of

$$q_c = \frac{\rho j^2}{V(1+\psi)} \frac{d}{4} \left(\frac{S_a}{S_t}\right)^{-1} \quad (1)$$

$$I = \frac{j}{1+\psi} \frac{n \pi d^2}{4} \quad (2)$$

where n is the number of strands and $\left(\frac{S_a}{S_t}\right)$ is

the fraction of total surface area available for heat transfer. For an uncompacted cabled conductor

Table 1 illustrates the results of this analysis for the four pool-cooled conductors. You will note that the j/j_c varies from 0.41 to 0.53. This is principally due to the fact that the conductor diameter, d , is designed to the nearest 0.001 inch. The thickness of insulation on each conductor was selected based upon the maximum tolerable temperature rise which can be permitted at the operating-current density. Since at a given field the Nb_3Sn conductors are very similar in operating characteristics to NbTi conductors but may cost considerably more to manufacture, conductors 3 and 4 are regarded economically infeasible.

Table 1
50 kA Pool Cooled Conductor Specifications

Specification	1	2	3	4
Peak Flux, Tesla	0.5	0.5	0.5	0.5
Material	Nb_3Sn	Nb_3Sn	Nb_3Sn	Nb_3Sn
Number of Strands	504	504	504	504
One Strand Diameter, inches	0.001	0.001	0.001	0.001
Insulated Strand Diameter, inches	0.004	0.004	0.004	0.004
Recovery Heat Flux, W/cm^2	0.2	0.2	0.2	0.2
Conductor Material	Nb_3Sn	Nb_3Sn	Nb_3Sn	Nb_3Sn
Conductor Resistivity	40	9.448	0.676	0.557
Conductor Current	49.70	49.70	49.70	49.70
Conductor Weight, kg/m	1.07	1.656	1.730	1.743
Conductor Length, m	100	100	100	100
Recovery Flux	0.2	0.2	0.2	0.2
Recovery Heat Flux, W/cm^2	0.2	0.2	0.2	0.2

The technical and economically viable pool-cooled conductors which remain are conductors 1 and 2. The cabled conductors can be manufactured using cabling techniques already available to the superconductor industry; however, the lattice braided conductors require the development of a braiding machine. Because the lattice braided conductors are vastly superior to cabled conductors in current density and porosity characteristics, we have selected the lattice braided conductors for the reference designs.

The goal in the study of forced-cooled conductor designs for ohmic-heating coils, has been to develop conductor concepts which have recovery heat fluxes of 0.2 W/cm^2 or greater, limited only by the manufacturing limitation of 0.001 inch radial build of conductor insulation. Accordingly, six 50-kA, forced-cooled conductors were evolved based upon Equations 1 and 2. Table 2 summarizes these results.

The two types of forced-cooled conductors are similar to those illustrated in Figures 1 and 2. The lattice braid is as shown in Figure 2, whereas, the cabled conductor is similar to the cable illustrated in Figure 1 but the elliptical mandrel has been removed.

Table 2
50 kA Forced Cooled Conductor Specifications

Both conductors are sandwiched in a manner to allow forced-cooling of the strands.

In general, the forced-cooled conductors have comparable or higher conductor operating-current densities than the pool-cooled conductors listed in Table 1. This is due to the higher recovery heat flux for which forced-cooled conductors can in principle be designed. However, one pays for this higher operating-current density through the pumping power required to circulate the helium. Thus, there is an economic trade-off of refrigeration cost versus conductor cost when comparing the forced-cooled and pool-cooled conductors.

Two reference conductors were selected from ten candidate conductors and are characterized in Table 3. These conductors were selected based upon operating-current density, manufacturing limitations and relative cost comparisons.

AC Loss Calculations

The ac losses in the ohmic-heating coil conductors have been calculated assuming a nonoptimized superconductor configuration. For the purpose of this analysis, the following assumptions were made about the conductor configuration:

- In the NbTi conductors, the superconducting filaments were assumed to be 10 microns in diameter which is typical of the present state-of-the-art.
- In the Nb₃Sn conductors, the superconducting filaments are assumed to be annular with an outside diameter of 3.5 microns and an inside diameter of 1.5 microns, which is again, typical of the present state-of-the-art.
- The filament bundle in the NbTi conductors is assumed to have a copper-to-NbTi ratio of one to one.
- The filament bundle in the Nb₃Sn conductors is assumed to contain a tantalum web, a matrix of copper and 3 wt% Sn in addition to the Nb₃Sn and Nb filaments. The ratio of nonsuperconductor-to-superconductor in this region is assumed to be three to one.

- The copper stabilizer intrinsic residual resistivity ratio (RRR) is assumed to be 100; therefore, in zero magnetic field $\rho_{Cu} = 1.7 \times 10^{-10} \Omega\text{-m}$.
- The CuSn bronze in the Nb₃Sn conductor is assumed to be 10 times more resistive than Cu with an RRR = 100 and independent of magnetic field, therefore, $\rho_{CuSn} = 1.7 \times 10^{-9} \Omega\text{-m}$.
- The filament twist is assumed to be ten times the strand diameter in all cases.

Based upon these assumptions, the ac losses were calculated for the two reference conductors. Table 3 summarizes these calculations and the reference conductor characteristics. In all cases, the predominant ac loss is eddy current loss in the copper stabilizer. This loss can be lowered by using CuNi webbed conductor. However, since the surface heat flux during the field pulses is between two and fourteen times smaller than the surface heat flux required for cryostability, this loss reduction has been ignored at this time. In the case of the pool-builing conductor concepts, this loss is significant to the operation of magnet since it determines the amount of bubbles present during operation and the cooling requirement. Whereas, in the forced-cooled conductor concept, this loss is most probably insignificant with respect to pumping power requirements to circulate the helium and provide cryostability.

Table 3
Reference 50 kA Conductor Characteristics and Coil Parameters

Category	Sub-Category	Definition	Example	Notes
Geometric Properties	Shape	Refers to the form or outline of an object.	Circle, square, triangle, rectangle.	
	Size	Refers to the dimensions or scale of an object.	Large, small, tall, short.	
Material Properties	Texture	Refers to the surface quality or feel of an object.	Smooth, rough, soft, hard.	
	Color	Refers to the visual appearance of an object.	Red, blue, green, yellow, purple.	
Functional Properties	Function	Refers to the purpose or use of an object.	Tool, toy, container, vehicle.	
	Material	Refers to the physical composition of an object.	Wood, metal, plastic, glass.	
Aesthetic Properties	Beauty	Refers to the pleasing or attractive qualities of an object.	Stylish, elegant, beautiful.	
	Attractiveness	Refers to the qualities that make an object appealing or attractive.	Attractive, attractive, attractive.	
Cultural Properties	Symbolism	Refers to the meaning or symbolism associated with an object.	Religious symbols, cultural artifacts.	
	Tradition	Refers to the historical or traditional significance of an object.	Traditional, traditional, traditional.	
Sensory Properties	Taste	Refers to the flavor or taste of an object.	Sweet, salty, sour, bitter.	
	Smell	Refers to the odor or fragrance of an object.	Fragrant, aromatic, pungent.	
Emotional Properties	Emotion	Refers to the emotional response or feeling evoked by an object.	Happy, sad, angry, scared.	
	Memory	Refers to the ability of an object to trigger or唤起 memory.	Memorable, nostalgic, evocative.	
Social Properties	Relationship	Refers to the social connections or interactions associated with an object.	Friendship, family, community.	
	Community	Refers to the social context or environment in which an object is used.	Community, community, community.	
Technological Properties	Technology	Refers to the use of technology or advanced materials in an object.	High-tech, futuristic, modern.	
	Functionality	Refers to the practicality or effectiveness of an object.	Functional, functional, functional.	
Cognitive Properties	Information	Refers to the knowledge or information contained in an object.	Educational, informative, informative.	
	Learning	Refers to the process of acquiring knowledge or information through an object.	Learning, learning, learning.	
Aesthetic Properties	Beauty	Refers to the pleasing or attractive qualities of an object.	Stylish, elegant, beautiful.	
	Attractiveness	Refers to the qualities that make an object appealing or attractive.	Attractive, attractive, attractive.	
Cultural Properties	Symbolism	Refers to the meaning or symbolism associated with an object.	Religious symbols, cultural artifacts.	
	Tradition	Refers to the historical or traditional significance of an object.	Traditional, traditional, traditional.	
Sensory Properties	Taste	Refers to the flavor or taste of an object.	Sweet, salty, sour, bitter.	
	Smell	Refers to the odor or fragrance of an object.	Fragrant, aromatic, pungent.	
Emotional Properties	Emotion	Refers to the emotional response or feeling evoked by an object.	Happy, sad, angry, scared.	
	Memory	Refers to the ability of an object to trigger or唤起 memory.	Memorable, nostalgic, evocative.	
Social Properties	Relationship	Refers to the social connections or interactions associated with an object.	Friendship, family, community.	
	Community	Refers to the social context or environment in which an object is used.	Community, community, community.	
Technological Properties	Technology	Refers to the use of technology or advanced materials in an object.	High-tech, futuristic, modern.	
	Functionality	Refers to the practicality or effectiveness of an object.	Functional, functional, functional.	
Cognitive Properties	Information	Refers to the knowledge or information contained in an object.	Educational, informative, informative.	
	Learning	Refers to the process of acquiring knowledge or information through an object.	Learning, learning, learning.	

Structural Design

The structural design must consider the following factors:

- Restraint of electromagnetic forces
- Conductor motion
- Conductor cooling

The structural design for both coils is based on the 300 kJ coil(2) that has been successfully tested at LASL when subjected to an ohmic-heating cycle(3). The pulsed operating cycle requires minimization of electrically conducting structures to minimize eddy current losses during the operating cycle. For this reason fiber reinforced composites were used wherever possible in the coil structure.

The structure design was developed using the following design codes:

- The maximum strain in the NbTi superconductor should be limited to 0.2%.
- The maximum strain in the Nb₃Sn superconductor should be limited to 0.1%.
- The primary stress intensity in the structure should be less than two-thirds material yield stress or 40% of ultimate stress whichever is less.
- The maximum stress theory will be used for composite structures.

The design concept for the coil is shown in Figure 3. The design, using forced convection cooling, differs from the pool-boil design in that the bubble migration and cooling channels are eliminated and the helium coolant is forced through the conductor itself. Both concepts use teeth to support axial forces and stainless steel bands for radial support. The axial and radial forces vary within the coil cross section. The structural design considers three areas: the tooth thickness, t_t , the banding thickness, t_B and the former thickness t_f .

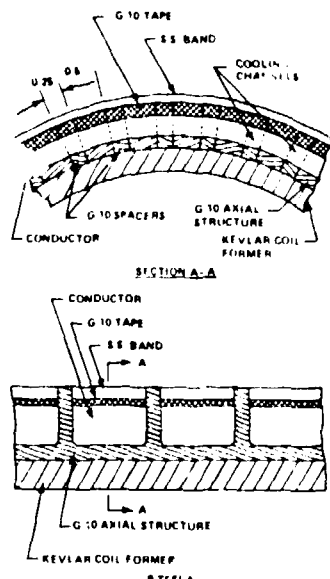


Figure 3 20 MJ Conceptual Design

Tooth Thickness

The tooth thickness was calculated based on a cantilever beam with uniform loading, w , in the axial direction. The axial spacers or tape can provide support at the tooth tip; however, it was assumed this could not be reliably achieved in manufacture. The tooth thickness, t_t , is given by

$$t_t = \frac{SM}{S} \quad (3)$$

$$\text{where } M = \frac{wL^2}{2}$$

$$\begin{aligned} S &= \text{design stress} \\ M &= \text{moment} \end{aligned}$$

The tooth width can be decreased from its maximum value at the coil ends toward the center as the axial force decreases. This structural grading can be accomplished continuously or in discreet steps. Either method would require a change in winding pitch as the teeth thicknesses were decreased. Although this is possible from a manufacturing standpoint, it would be expensive. For this reason the tooth width was held constant at the maximum thickness required to support the maximum axial force.

Banding Thickness

The banding thickness, t_B , can also be varied due to the variation of radial forces. The concept uses an overwind of metal banding on the conductor outside surface. The thickness will be varied to limit the strain in the conductor to prevent degradation of its current carrying capacity. The band will be fastened at each end of each layer. This will enable tension to be developed within the band without providing circumferential electrical conductivity which would result in significant electrical losses during pulsed operation. The membrane stress in the band is given

$$\text{by } S = \frac{PR}{t_B} \quad (4)$$

$$\text{or } t_B = \frac{PR}{S}$$

Former Thickness

The former thickness, t_f , is sized to achieve the required pre-stress during cooldown to minimize conductor motion. When the coil is energized, the compression is relieved as the magnetic force in the conductor increases. This results in a relatively constant tension in the banding until the magnetic forces exceed the pre-load forces. This concept was used successfully in the 300 kJ coil using the following technique.

Since both the initial and final (deformed) positions will be coincident, the total radial deflection (due to thermal contraction and stress) will be equal for the conductor and the coil former:

$$R = R \alpha \Delta T + \frac{\sigma_t}{E} \text{cond} = R \left(\alpha \Delta T + \frac{t}{E} \right) \text{former} \quad (5)$$

where

R = radius common to conductor and former (in.)

α = thermal contraction coefficient (in/in $^{\circ}$ F)

t = temperature change (negative, $^{\circ}$ F)

σ_t = hoop tensile stress (psi)

E = elastic modulus (psi)

Also, it can be shown from a force-balance, that the tensile force in the conductor ($A \times \sigma_t$)_{cond} must be equal and opposite to that in the coil former, for equilibrium, so that (using subscripts "1" for the conductor and "2" for the former):

$$\frac{\sigma_t}{t_1} = -\frac{\sigma_t}{t_2} \quad (6)$$

Equations 5 and 6 may be combined to show:

$$\frac{\sigma_t}{t_1} = \frac{(a_2 - a_1) \Delta T}{T/E_1 + A_1/(A_2 E_2)} \quad (7)$$

$$\frac{\sigma_t}{t_2} = \frac{(a_1 - a_2) \Delta T}{T/E_2 + A_2/(A_1 E_1)} \quad (8)$$

As seen, the pre-stress in both the band and former are dependent upon the physical and mechanical properties of the two sub-assemblies. The technique assumes an infinitely rigid conductor as was the case in the 300 kJ analysis. The analysis technique can be modified to include the conductor flexibility when available. The concept also assumed that each layer acts independently. The former thickness, t_f , can be structurally graded for each layer; however, for this conceptual study, a constant thickness was chosen for every layer to achieve a uniform current distribution in the coil cross section.

Using the design criterion specified above, the tooth thickness, t_t , was calculated at 0.71 inches. The maximum bending stress was 5600 psi (40% of 14,000) assuming an axial alignment of fibers. This calculation does not include the reinforcement at the tooth root provided by the conductor shape. The shear stress was calculated as 912 psi, which is 1/3 of the allowable interlaminar shear strength. The tooth thickness, t_t , can be reduced further if a radial fiber orientation could be achieved in the tooth. However, the larger tooth was used in the interest of conservative design.

The radial strain for the design was limited to 0.2% resulting in a hoop stress in the stainless steel band of 28,400 psi. The variation of banding thickness with radius to achieve this strain is shown in Figure 4. Using this banding thickness and a former thickness of 0.42, the banding pre-stress due to cooldown was calculated and the results are shown in Figure 4.

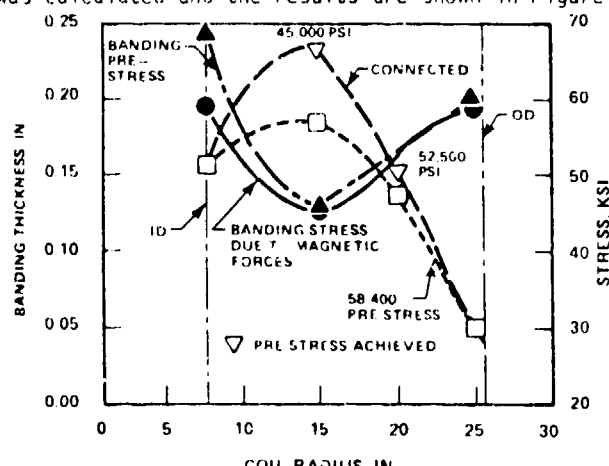


Figure 4 Variation of Band Thickness and Banding Stress with Radius

Calculation of the pre-stress using this variation of banding width indicated that the proper pre-stress to prevent conductor motion could not be achieved. The pre-stress induced during cooldown was less than that achieved upon coil energization raising the possibility of gaps developing between the conductor and former or between the conductor and banding. To eliminate this possibility the banding thickness was changed to the corrected curve also shown on Figure 4.

The banding stress due to magnetic forces and cooldown pre-stress are shown in Figure 4 as a function of radius. A good match between the two values was achieved over the entire radius thus providing a coil with minimal layer-to-layer motion while preventing the formation of undesirable gaps in the conductor support.

The axial structures are bonded to the formers using polyurethane adhesion because polyurethane adhesives are the most appropriate for use at cryogenic temperature(1)&(5). This is so because they share the least embrittlement at very low temperatures compared to other classes of adhesives. They can be cured at room temperatures and do not need much pressure during cure.

Cooldown Stresses

An analysis was performed to estimate the stresses that are developed during cooldown. The analysis was based on the assumption that the coil will be cooled to near 77K using liquid nitrogen. The potential for high stress exists due to differentially cooling portions of the winding. The cooldown stresses have been evaluated for three major assemblies:

- The coil tie studs
- The coil formers and banding
- The composite support tube

The stresses in the tie studs were calculated based on the assumption that the coil was at 300K and the studs at 77K. The tensile stress induced in the studs is 6200 psi which is well below the allowable stress of 22,000 psi (40% of 55,000 psi) for this material.

The stress induced in the banding and former was calculated based on the thermal shrink fit analysis. It was assumed that the banding was cooled to 77K with the former maintained at 300K.

The maximum stresses for the design were 75,400 psi for the banding and -33,700 psi for the former. Using this very conservative assumption, all stresses are below the material yield stress thus preventing any relaxation in the coil structure that could produce gaps during operation.

The stress in the 3 in. thick composite support tube were calculated using the technique developed for the 300 kJ coil⁽²⁾.

Across an inner cylinder maximum thickness of 3.0 in., the temperature difference would be 84K (329F). For a linear temperature profile, the maximum thermal stress at the surface is $\sigma = E \times T/2$. Using material properties in the plane of the filaments the computed thermal stress is much less than the design strength of the composite material.

Cyclic Stresses

The pulse cycle of 10 to 100 sec. requires 3.14×10^5 to 3.14×10^6 cycles per year of continuous operation. For a 20 year life-time this would require a fatigue life of 6.28×10^6 to 6.28×10^7 total cycles. The cooldown and warmup cycles, it is anticipated, would be in the range of 1000 cycles, based on one cycle per week for twenty years.

In considering the cyclic stresses three areas must be evaluated.

- Stainless steel banding
- Coil formers
- Axial structure

The stainless steel banding and coil formers are subjected to similar cyclic loads. During cooldown, the band stress increases from near zero to its maximum tensile value. The coil former stress increases from near zero to its maximum compressive stress. The stresses in banding are fairly uniform during pulsed operation because of the pre-stressed design concept was used. The stress in the coil former will decrease as the pre-load is dissipated by the magnetic forces. A Goodman diagram for cold rolled 304 stainless steel bar is shown on Figure 5 based on material properties of Reference 7. The mean stress intercept is taken as the material's ultimate strength. The maximum range stress, at zero mean stress was taken at $0.5 S_e$ ⁽⁶⁾. For the coil, during cooldown, the mean and range stress are identical at 30 ksi. This is Point A on Figure 5 well within acceptable range for 1000 cycles. During pulsed operation, the maximum mean stress in the banding will be of the order of 60 ksi. The allowable range stress for a fatigue life of 10^7 cycles is shown as Point B on Figure 5, 40 ksi or a maximum band tensile stress of 100 ksi. The 60 ksi pre-load stress due to cooldown will not be exceeded, therefore the banding will withstand 10^7 cycles of pulse operation.

The fatigue properties of the KEVLAR composite are not known at liquid helium temperatures; however, most composite material properties remain the same or improve as the temperature is lowered. The maximum stress in the KEVLAR former is 17.7 ksi developed during cooldown. As the coil is energized, this value will decrease to near zero due to the action of the magnetic forces. The tensile fatigue properties of KEVLAR are excellent. In tensile-tensile fatigue tests, a fatigue life of 10^7 cycles can be achieved at 70% of ultimate stress⁽⁷⁾. This factor was applied to the compressive ultimate stress at room temperature to establish an endurance limit.

The maximum cyclic stress in the coil former for the two designs were plotted on a Goodman diagram to determine the factor of safety. The results are shown in Figure 6. For the coil the factor of safety on the room temperature endurance limit is 2.5 based on 70% of the material ultimate strength. The total safety factor based on published data is 3.57. The maximum stresses in the coil former are within the design criterion of 40% of ultimate strength based on room temperature properties. This maximum stress is higher than the design objective for the structural design assuming room temperature properties.

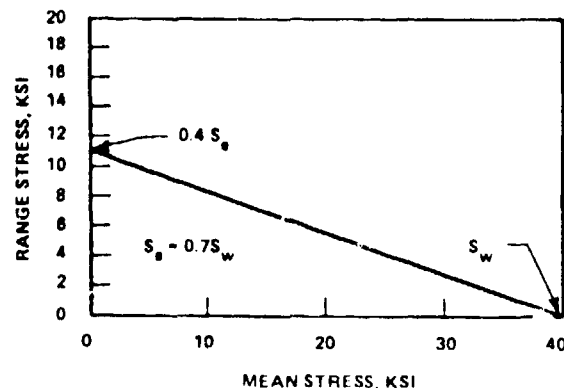


Figure 6 Goodman Diagram for KEVLAR Formers

Some data are available indicating that the compressive strength of KEVLAR is higher at 4.2K⁽⁶⁾. Therefore the material properties should be tested at 4.2K prior to commitment of a final design.

The stresses on the axial structure occur only during pulsing. The bending stresses were limited to 40% of the transverse strength. This criterion was used on the 300 kJ coil. This assumes that the bending and shear stress is supported by the composite matrix. This represents a conservative approach since radial fiber orientation would significantly increase the bending strength of the teeth. The longitudinal fatigue strength of epoxy fiberglass composites range from 23 to 45 ksi at 10^7 cycles at 4.2K⁽⁸⁾. The transverse fatigue properties of composites is not known at 4.2K. Prior to commitment of a final design, the transverse fatigue strength of the composite should be established. If the fatigue strength is insufficient, the axial structure should be modified for radial fiber orientation.

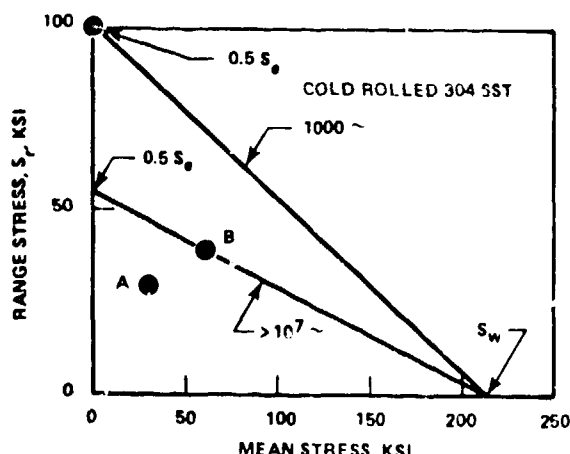


Figure 5 Goodman Diagram for SST Banding

Conclusions

The design demonstrates the feasibility of the ohmic-heating coil. The structural analysis shows that enough structure is provided to withstand the Lorenz force and the design concept minimizes the conductor motion during coil energization. The overall coil design meets or exceeds all the performance requirements. The reliability and manufacturability of the coil has been demonstrated on the Westinghouse 300 kJ coil. At the present time the Westinghouse Electric Corporation is involved with the detailed design and analysis of the 20 MJ superconducting ohmic-heating coil, incorporating a different set of design specifications. The results of the detailed design phase of this program will be reported later.

References

1. Singh, S. K.; Murphy, J. H.; Janocko, M. A.; Haller, H. E.; Riemersma, H.; Vota, T. L.; Litz, D. C.; Gromada, R.; Eckels, P. W.; Sanjana, Z. N.; Domeisen, F. N.; "Prototype Tokamak Ohmic-Heating 20 MJ Superconducting Coil Study," Part II - Technical Report, Contract No. L-48-8407C-1 April 1978.
2. Mullan, E., et al., "Design and Fabrication of 300 kJ Superconducting Energy Storage Coil," E.M. 5077, Subcontract No. XN4-32767-3, July 1977.
3. Thullen, P., et al., "Superconducting Ohmic-Heating Coil Simulation," Applied Superconductivity Conference, Pittsburgh, Pennsylvania, 1978.
4. Janocko, M.A., "Lattice Braided Superconductors," Applied Superconducting Conference, Pittsburgh, Pennsylvania, 1978.
5. Miska, K. H., "Which Low Temperature Adhesive is best for you?", Materials Engineering, May 1975, pp 52-54.
6. McLaughlin, J. R., "Low Temperature Properties of High Performance Composites," Technical Conference, Reinforced Plastics/Composites Institute, The Society of the Plastics Industry, 1975.
7. "KEVLAR-49 Data Manual", E. I. DuPont de Nemours
8. Kasen, M. B., "Mechanical and Thermal Properties of Filamented-Reinforced Structural Composites at Cryogenic Temperatures", ARPA Order No. 2569.